Lipopolysaccharide Induces Type 2 Iodothyronine Deiodinase in the Mediobasal Hypothalamus: Implications for the Nonthyroidal Illness Syndrome

CSABA FEKETE, BALÁZS GEREBEN, MÁRTON DOLESCHALL, JOHN W. HARNEY,
JOSE MIGUEL DORA, ANTONIO C. BIANCO, SUMIT SARKAR, ZSOLT LIPOSITS, WILLIAM RAND,
CHARLES EMERSON, IMRE KACSKOVICS, P. REED LARSEN, AND RONALD M. LECHAN

Department of Endocrine and Behavioral Neurobiology (C.F., B.G., Z.L.), Institute of Experimental Medicine, Hungarian Academy of Sciences, Budapest H-1083; Department of Physiology and Biochemistry (M.D., I.K.), Faculty of Veterinary Science, Szent István University, H-1400 Budapest, Hungary; Thyroid Section (J.W.H., J.M.D., A.C.B., P.R.L.), Division of Endocrinology, Diabetes and Hypertension, Brigham and Women's Hospital and Harvard Medical School, Boston, Massachusetts 02115; Tupper Research Institute and Department of Medicine (S.S., R.M.L.), Division of Endocrinology, Diabetes, and Metabolism, Tufts-New England Medical Center, Boston, Massachusetts 02111; Department of Community Health (W.R.) and Department of Neuroscience (R.M.L.), Tufts University School of Medicine, Boston, Massachusetts 02111; and Division of Endocrinology (C.E.), University of Massachusetts Medical School, Worcester, Massachusetts 01655

To determine whether the type 2 iodothyronine deiodinase (D2), the principal central nervous system enzyme converting T_4 to biologically active T_3, is regulated in tanycytes by immune activation, D2 activity was measured in the mediobasal hypothalamus (MBH) 4, 12, and 24 h after administration of bacterial lipopolysaccharide (LPS) and compared with D2 levels in the cortex and anterior pituitary of rats. In contrast to D2 activity in the cortex and anterior pituitary that showed a steady linear increase over 24 h, which was coincident with a decline in thyroid hormone and TSH levels, D2 activity peaked in the MBH 12 h after LPS administration. By *in situ* hybridization, the increased D2 mRNA synthesis induced by LPS was specifically localized to tanycytes lining the third ventricle. *In vitro* assays in HC11 and HEK-293 cells demonstrated that the p65 subunit of nuclear factor-κB markedly increased both rat and human D2 genes (*dio*2) as analyzed by promoter assays. No activation of human *dio*2 was observed when an 83-bp minimal promoter was used. We propose that LPS or LPS-induced cytokines directly induce D2 mRNA in tanycytes. The ensuing MBH-specific D2-mediated local thyrotoxicosis may suppress the hypothalamus-pituitary-thyroid axis by local feedback inhibition of hypophysiotropic TRH and/or TSH and contribute to the mechanism of central hypothyroidism associated with infection. (*Endocrinology* **145:** 1649–1655, 2004)

TYPE 2 IODOTHYRONINE DEIODINASE (D2) is one of three known iodothyronine deiodinases and the predominant outer ring deiodinase in the brain catalyzing the intracellular generation of T_3 from T_4 (1). Because greater than 75% of nuclear T_3 in the brain is derived from local conversion of T_4 to T_3 (1), D2 has an essential role in mediating the effects of circulating thyroid hormone on the central nervous system (1). The conversion of T_4 to T_3 within the brain is also an important component of the inhibitory feedback mechanism of thyroid hormone on TRH-synthesizing neurons in the hypothalamic paraventricular nucleus (PVN) that are involved in the regulation of TSH secretion (2). This is based on the observation that the systemic administration of T_3 to hypothyroid animals reduces TRH mRNA in the PVN to normal only when abnormally high peripheral T_3 levels are attained (2). In addition, mice with targeted disruption of the D2 gene (*dio*2) have increased serum T_4 and TSH concentrations, characterizing a state of relative resis-

tance of the hypothalamic-pituitary axis to inhibition by T_4 (3).

Recent studies in our laboratories have demonstrated that tanycytes express one of the highest concentrations of D2 activity and D2 mRNA in the brain (4). Tanycytes are specialized ependymal cells of glial origin that line the floor and ventrolateral walls of the third ventricle between the rostral and caudal limits of the hypothalamic median eminence (5, 6). Characteristic of tanycytes are apical microvilli and stereocilia that extend into the cerebrospinal fluid (CSF), and a basal process that ramifies into the underlying neuropil, encircling blood vessels in the adjacent arcuate nucleus and terminating in numerous endfeet processes on or near fenestrated capillaries of the primary portal plexus in the external zone of the median eminence (5). Thus, tanycytes may provide a bidirectional, cytoplasmic conduit between the CSF in the third ventricle and the blood in the vascular elements of the arcuate nucleus and/or median eminence, allowing the movement of substances from one compartment to the other. Because D2 activity and D2 mRNA are not present in the hypothalamic PVN (4), it has been hypothesized that T_4 to T_3 conversion by D2-expressing tanycytes may participate in feedback regulation of the hypothalamic-pituitary-thyroid axis after uptake of T_4 by tanycytes from CSF or vascular compart-

ments and release of T_3 back into the CSF, bloodstream, or median eminence (4).

On the basis of recent observations that tanycytes increase their expression of TNF-1 (p55) receptors in response to endotoxin (7) and express macrophage migration inhibitory factor (8), we have raised the possibility that tanycytes may serve as an important interface between the peripheral immune system and the brain to regulate specific neuroendocrine systems. Therefore, in the present study, we determined whether D2 activity and *dio*2 expression are increased in tanycytes after immune activation using the systemic administration of bacterial lipopolysaccharide (LPS) as a model system. Because TNF-α is thought to signal primarily by the activation of nuclear factor-κB (NF-κB) (9, 10), we determined whether p65 (RelA), a required component of NF-κB signaling (10), mediates transactivation of *dio*2 in HC11 and HEK-293 cells.

Materials and Methods

Animals

The experiments were carried out on adult male Sprague Dawley rats (Taconic Farms, Germantown, NY) weighing 210–230 g. The animals were housed individually in cages under standard environmental conditions (light between 0600–1800 h, temperature 22 $\pm$ 1 C, and rat chow and water *ad libitum*). All experimental protocols were reviewed and approved by the Animal Welfare Committees at the New England Medical Center, Tufts University School of Medicine, and the Institute of Experimental Medicine.

Animal and tissue preparation for D2 analysis

Rats were divided into four groups (n = 32, eight animals per group). Three groups were injected ip with 250 μg per 100 g of body weight (BW) bacterial LPS (Sigma O127:B8; Sigma Chemical Co., St. Louis, MO) in saline. The fourth group received only vehicle and was used as control. Rectal temperature was taken before and every 2 h after the injections. LPS-treated groups were anesthetized with pentobarbital (50 mg/kg BW ip) 4, 12, and 24 h after LPS administration. Blood was taken from inferior vena cava for measurement of serum T_4, T_3, and TSH, and the animals were decapitated. The brain was removed from the skull, and a strip of cortex and an approximately 2-mm diameter cube of mediobasal hypothalamus (MBH) were rapidly dissected with a scalpel and iridectomy scissors and frozen in an Eppendorf tube on dry ice. The pituitary gland was removed from the sella turcica, and the anterior lobe was separated from the intermediate and posterior lobes before freezing as above. Because our preliminary data indicated that changes in D2 activity in the MBH are highest 12 h after LPS administration, the control group was anesthetized and dissected 12 h after saline administration.

Animal and tissue preparation for in situ hybridization

Two groups of animals were studied (n = 10). Five animals were injected ip with 250 μg/100 g BW LPS in saline, and five were injected with saline. Twelve hours after the injections, the animals were anesthetized with sodium pentobarbital (50 mg/kg BW ip) and immediately perfused transcardially with 20 ml of 0.01 M PBS (pH 7.4) containing 15,000 U/liter heparin sulfate followed by 150 ml 4% paraformaldehyde in PBS. The tissues were prepared for *in situ* hybridization as described earlier (11).

Real-time RT-PCR

The MBH of three LPS and four saline-treated control rats were pooled, and total RNA was isolated followed by cDNA synthesis. Real Time RT-PCR was performed using a Roche LightCycler (Roche Applied Science, Mannheim, Germany) according to the manufacturer's instructions using the LightCycler DNA Master SYBR Green I kit. All reactions

were run in triplicate in three separate experiments using intron spanning primers for D2 and β-actin as an internal control. The results are expressed as the fold change of D2 to β-actin mRNA ratios in LPS-treated animals compared with that of controls.

D2 measurements

D2 activity was measured as described (12). Fifty to 100 μg total tissue sonicate protein were incubated at 37 C for 2 h in the presence of 1 nM [^{125}I]5'-T_4, 20 mM dithiothreitol, and 1 mM 6-n propylthiouracil. Specific T_4 to T_3 conversion was calculated by subtracting nonspecific deiodination in tubes containing similar amounts of lysate protein obtained from HEK-293 cells that have no deiodinase activity. The background activity of these samples was less than 2%. Deiodinase activity was expressed as fmol T_4/min/mg protein.

Hormone measurements in sera

Thyroid hormones and TSH measurements were performed by RIA as described (11).

In situ hybridization histochemistry

Every fourth section was hybridized with a 800-bp, single-stranded, [^{35}S]UTP-labeled cRNA probe complementary to the entire coding region of the rat D2 gene. The hybridization was performed as described previously (11). Slides were dipped into Kodak NTB2 autoradiography emulsion (Eastman Kodak, Rochester, NY), and the autoradiograms were developed after 4 d of exposure at 4 C. The specificity of hybridization was confirmed using sense probes, which resulted in the total absence of specific hybridization signal in the hypothalamus.

Image analysis

Autoradiograms were visualized under darkfield illumination using a COHU 4910 video camera (COHU, Inc., San Diego, CA), and the images were analyzed with a Macintosh G4 computer (Apple Computers Inc., Sunnyvale, CA) using Scion *Image* (Scion Corp., Frederick, MD). Background density points were removed by thresholding the image. Integrated density values (density $\times$ area) of the hybridized region in the MBH were measured in one group of slides of 12 consecutive sections for each animal, beginning with the most rostral portion of the median eminence. Nonlinearity of radioactivity in the emulsion was evaluated by comparing density values with a calibration curve created from autoradiograms of known dilutions of the radiolabeled probes that were immobilized on glass slides in 1.5% gelatin, fixed with 4% formaldehyde, and exposed and developed simultaneously with the *in situ* hybridization autoradiograms.

DNA constructs and in vitro analysis of the D2 promoter

Approximately 6.9 kb of the human *dio*2 (h*dio*2) 5' flanking region (FR; h*dio*2-6.9-Luc; $\sim$−6.9 to +7 relative to the 5' transcriptional start site) and its 3' fragments (h*dio*2-2.1-Luc and h*dio*2-584-Luc; $\sim$−2.1 to +7 and −584 to +7, respectively) were cloned into pGL3Basic firefly luciferase reporter plasmid (Promega Corp., Madison, WI) using an approximately 110-bp linker located 3' to the +7 *Pst*I site in the h*dio*2 5' untranslated region. The linker was the *Pst*I-*Nhe*I no ATG-containing reverse complementer region of chicken D2 5' untranslated region (GenBank accession no. AF125575). The *dio*2 (r*dio*2) Luc construct (r*dio*2-3.6-Luc) was kindly donated by Dr. S. W. Kim (Brigham and Women's Hospital and Harvard Medical School, Boston, MA). It contains the *Bcl*I-*Bsr*BI region ($\sim$−3.6 kb to +85) of r*dio*2.

Sequences of the h*dio*2 5'FR and r*dio*2 5'FR have been previously described (13, 14). HC11 cells were cultured as described (15) and transfected by the polyethylenimine method (16). Two hundred nanograms of the pGL3Basic constructs were cotransfected with 150 ng of a cytomegalovirus promoter-driven p65 expression vector (17) or the same amount of the empty pCI-Neo vector (cytomegalovirus promoter; Promega). To monitor transfection efficiency, 4 ng pRL-SV40 *Renilla* luciferase (Promega) was transfected, accompanied by 1250 ng

pUC19 carrier DNA. The given DNA amounts refer to a dish of 15.6 mm in diameter (24-well plate). Luciferase activity of three separate transfections were determined in triplicates using the Dual-Luciferase Reporter Assay System (Promega) and a Luminoskan Ascent luminometer (Thermo Labsystems, Vantaa, Finland). In our hands, *Renilla* luciferase expression of the pRL-SV40 vector was consistently 3-fold down-regulated by p65. Therefore, the Luciferase to *Renilla* ratio of p65 transfected cells was divided by three to obtain the true induction ratio.

Transfections of HEK-293 cells were performed with calcium phosphate-DNA precipitates using an internal thymidine kinase human GH control for transfection efficiency as previously described (18). Chloramphenicol acetyl transferase (CAT) assays were performed by the method of Seed and Sheen (19), and the results are expressed as the ratio of cellular CAT to medium human GH (20). HEK-293 cells were transfected with 200 ng p65/60 mm dish and 5 μg of h*dio2*-6.5-CAT, h*dio2*-610-CAT, or h*dio2*-83-CAT constructs containing a 6.5-kb, 3' 610-bp, and 3' 83-bp long *dio2* 5' FR 5' to a CAT reporter, respectively, as described (13, 14).

Statistical analysis

Results are presented as means ± se (sem). The data of the hormone measurements and *in situ* hybridization analyses were compared with one-way ANOVA followed by Newman-Keuls *post hoc* testing. Data were entered into and analyzed using SPSS version 11.5 (SPSS Inc., Chicago, IL). Promoter analysis was statistically evaluated by the unpaired *t* test or one-way ANOVA followed by Newman-Keuls *post hoc* testing. $P < 0.05$ was considered statistically significant.

Results

Effect of LPS administration on temperature and plasma hormone levels

LPS-treated animals had a small reduction in rectal temperature compared with controls 4 h after administration (control *vs.* 4-h LPS: 37.8 ± 0.1 *vs.* 37.1 ± 0.3 C) that rose into the supranormal range at 12 and 24 h after LPS to 38.1 ± 0.1 and 38.2 ± 0.1 C, respectively. In addition, animals receiving LPS were readily distinguished from control animals by their behavioral changes; they became quiescent in their cages within 4 h of administration and developed a characteristic reddening of their tails due to vasodilatation.

Circulating thyroid hormone (T_3 and T_4) and TSH levels were markedly reduced by LPS (Fig. 1, A–C). The fall for T_3, T_4, and TSH values was highly correlated with time, reaching its nadir at 24 h (r = −0.63, −0.68, and −0.52, respectively; $P < 0.01$).

Effect of LPS administration on D2 activity

D2 activity in the anterior pituitary and cortex was increased by the administration of LPS, reaching maximal levels at 24 h ($F_{(3,28)} = 3.562$, $P = 0.027$; $F_{(3,28)} = 4.826$, $P = 0.008$, respectively; Fig. 1D). In contrast, D2 activity in the MBH
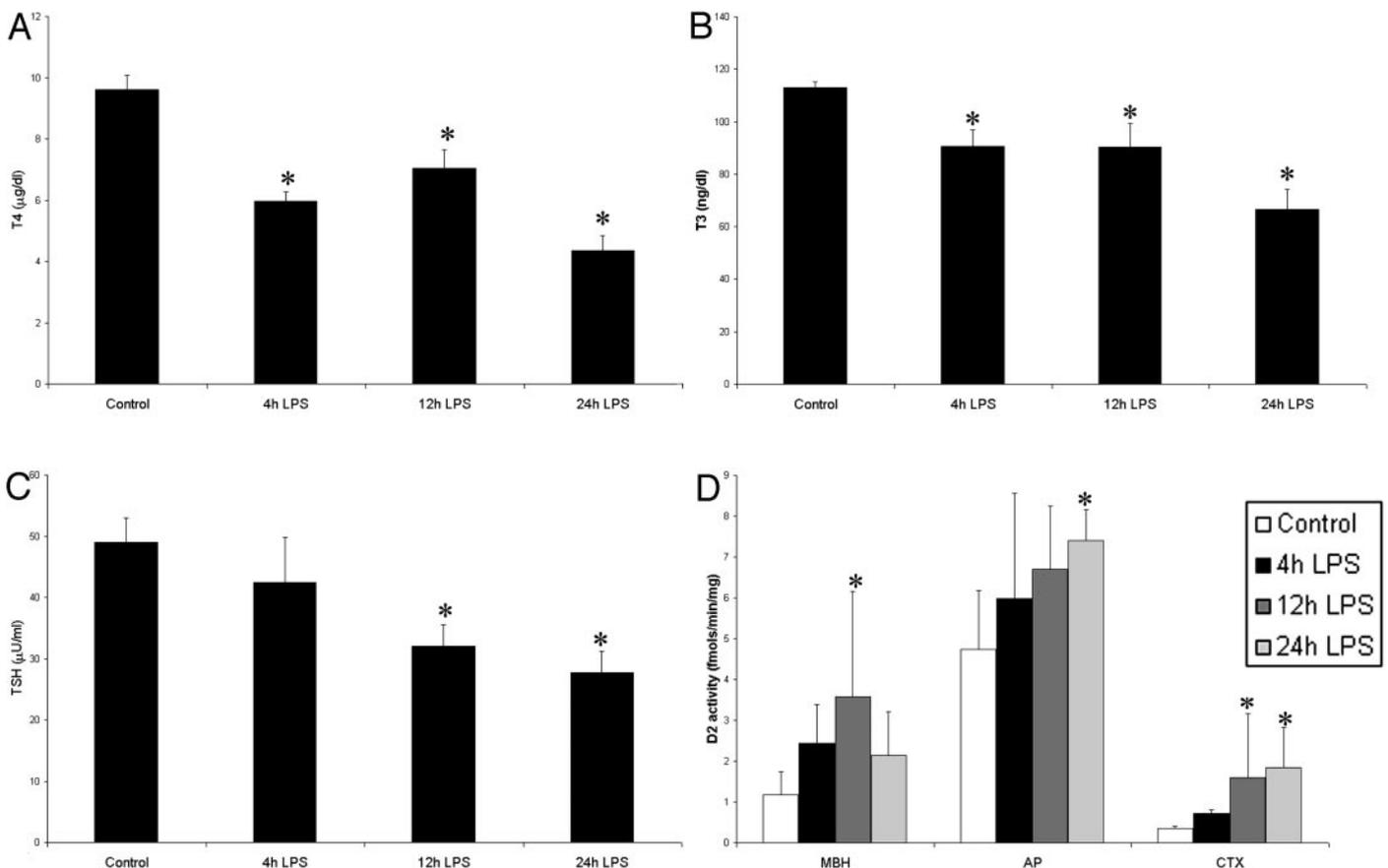

FIG. 1. Effects of ip bacterial LPS administration (250 μg/100 g BW) on (A) T_4, (B) T_3, and (C) TSH levels, and (D) D2 activity in the anterior pituitary (AP), cerebral cortex (CTX), and MBH of Sprague Dawley rats. Plasma T_3, T_4, and TSH levels are lowest at 24 h after LPS treatment. Although D2 activity in the cortex and anterior pituitary shows a steady linear increase over time, peak activity in the MBH occurred 12 h after LPS administration, before the maximal decline in thyroid hormone levels. *, $P < 0.05$ compared with baseline.

reached its peak activity at 12 h after LPS ($F_{(3,28)} = 3.502$, $P = 0.028$).

Effect of LPS administration on D2 mRNA levels in the MBH

D2 mRNA was readily visualized in the MBH, contained within cells densely clustered within the floor and infralateral walls of the third ventricle (Fig. 2, A–H). Characteristic of tanycytes, D2 mRNA extended into the processes of these cells, terminating in the adjacent arcuate nucleus surrounding blood vessels and also projecting toward the tuberoinfundibular sulcus and the median eminence. Within the median eminence, D2 mRNA localized primarily in the outer portion of the external zone. Twelve hours after LPS administration, D2 mRNA levels markedly increased, particularly in the external zone of the median eminence (Fig. 2, E–H). By image analysis, LPS administration induced an approximately 2.5-fold increase in the density values of silver grains over tanycytes, which was significantly different from controls (Fig. 3).

Refinement of D2 mRNA quantitation in the MBH 12 h after LPS administration was performed by real-time RT-PCR and showed a 3.71 ± 0.54-fold increase in the D2 to β-actin mRNA ratios of LPS-treated animals compared with controls.

Effect of p65 (RelA) on the rdio2 and hdio2 promoter

In HC11 cells, coexpression of p65 with the r*dio*2-3.6-Luc constructs increased the transcriptional activity of the r*dio*2 gene 2.9-fold (Fig. 4A) and in a very robust induction of h*dio*2-Luc constructs. The 6.9-kb h*dio*2 5′FR fragment (h*dio*2-6.9-Luc) was induced 152-fold, whereas removing its 5′ 4.8-kb fragment reduced the response of the remaining 2.1-kb 3′ region (h*dio*2-2.1-Luc) to 48-fold (Fig. 4B). The 584-bp long 3′ portion of the h*dio*2 5′FR (h*dio*2-584-Luc) responded 38-

fold, whereas the only-linker-pGL3basic vector could not be induced by p65 overexpression.

In HEK-293 cells, p65 induced the h*dio*2-6.5-CAT 56-fold, whereas the 3′ 610-bp long fragment of the promoter (h*dio*2-610-CAT) showed only a 17-fold induction (Fig 4C). The 83-bp long D2 minimal promoter (h*dio*2-83-CAT) remained unresponsive (Fig. 4C).

Discussion

These studies demonstrate that D2 activity in the MBH is substantially increased by immune activation. After an ip injection of LPS, D2 activity in the MBH showed an early maximal response at 12 h, followed by a decline at 24 h. The response was exclusive to tanycytes, and by semiquantitative *in situ* hybridization histochemistry and real-time PCR, it
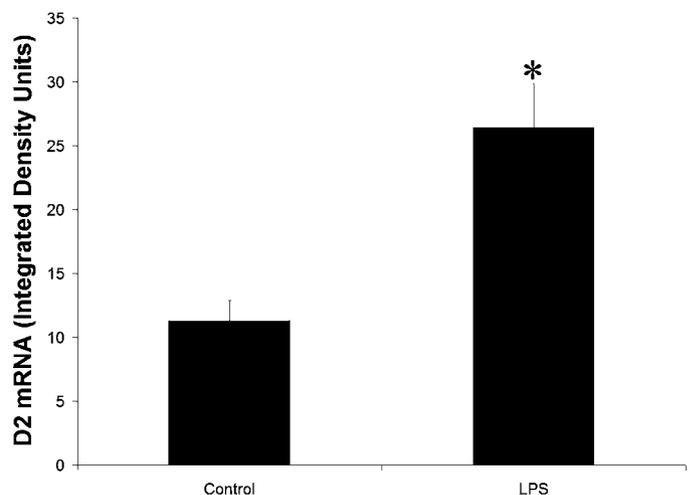

FIG. 3. Computerized image analysis of D2 mRNA content in the median eminence of control and LPS-treated animals. *, $P < 0.01$ compared with control.
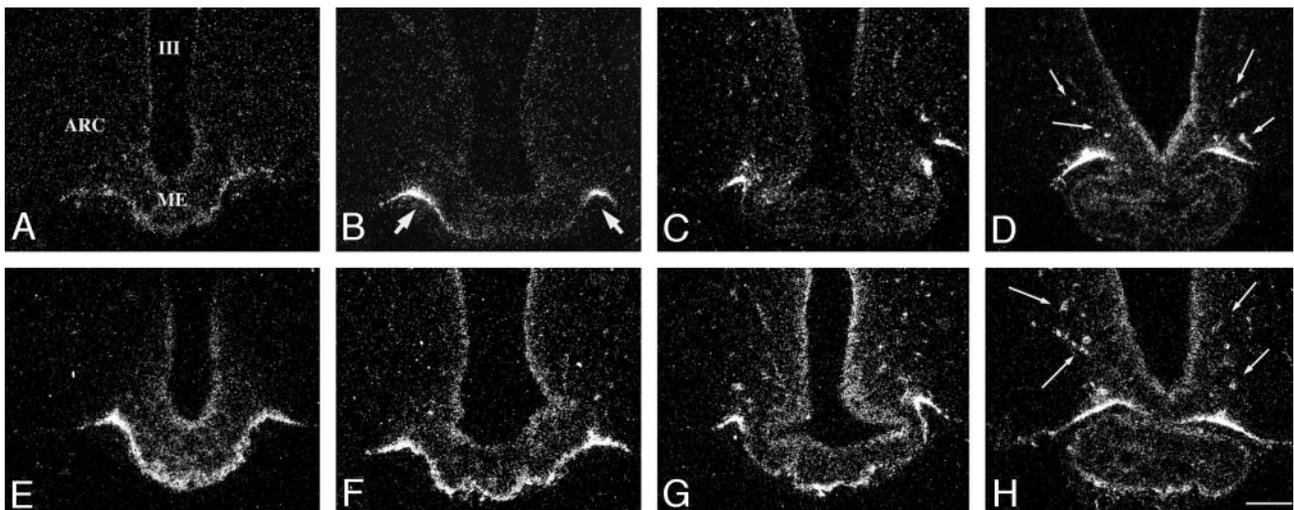

FIG. 2. Low-power dark-field micrographs from four different rostrocaudal levels of the median eminence (ME) showing the effect of LPS treatment on D2 gene expression in the MBH. A–D, Controls; E–H, LPS-treated animals. *Silver grains* denoting D2 mRNA are accumulated over cells lining the wall of the third ventricle (III), the tuberoinfundibular sulci (*arrow heads*), surround blood vessels (*arrows*) in the arcuate nucleus (ARC) and accumulate in the external zone of the ME. After LPS administration, the density of *silver grains* denoting D2 mRNA is markedly increased, particularly in the external zone of the ME (E–H). *Scale bar*, 200 μm.
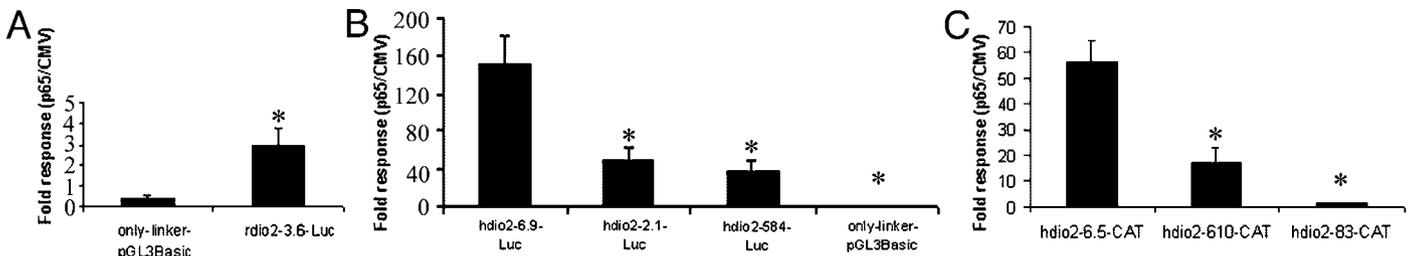
FIG. 4. Effect of the p65 NF-κB subunit on the activity of the r*dio*2 and h*dio*2 promoter in HC11 and HEK cells. Results are shown as the ratio of reporter expression (corrected for transfection efficiency) in the presence and absence of p65 (p65/cytomegalovirus). The ratios in experiments using the *Renilla* construct were divided by three to correct for the suppression of SV40-*Renilla* by p65 (see *Materials and Methods*). A, The r*dio*2-3.6-Luc construct containing approximately 3.6-kb r*dio*2 5′FR was induced 2.9-fold by p65 in HC11 cells. *, Significantly different from the activation of only-linker-pGL3 basic vector, $P < 0.05$. B, h*dio*2-584-Luc (containing the 3′ ~584 bp of the h*dio*2 5′FR), h*dio*2-2.1-Luc (containing the 3′ ~2.1 kb of the h*dio*2 5′FR), and h*dio*2-6.9-Luc (containing ~6.9 kb of the h*dio*2 5′FR) respond to p65 38-, 48-, and 152-fold, respectively. Activation of h*dio*2-584-Luc and h*dio*2-2.1-Luc constructs is significantly less then activation of h*dio*2-6.9-Luc. *, Significantly different from the activation of h*dio*2-6.9-Luc, $P < 0.01$. C, h*dio*2-6.5-CAT construct (containing ~6.5 kb of the h*dio*2 5′FR) and h*dio*2-610-CAT (containing 610 bp of the h*dio*2 5′FR) were induced 56- and 17-fold, respectively, by p65 cotransfection in HEK-293 cells. The h*dio*2-83-CAT containing the 83-bp long minimal D2 promoter remained unresponsive to p65. Activation of h*dio*2-610-CAT and h*dio*2-83-CAT was significantly less then activation of h*dio*2-6.5-CAT. *, Significantly different from the activation of h*dio*2-6.5-CAT vector, $P < 0.01$. Data are shown as the mean of response ± SEM of at least four separate experiments based on Luc to *Renilla* or CAT to human GH ratios.

increased nearly 4-fold compared with control animals. Because the pattern of D2 activation in tanycytes after LPS differed from the more gradual, linear or stepwise increase in D2 activity in the anterior pituitary and cortex that was maximal at 24 h, coincident with the maximal fall in circulating thyroid hormone levels, we presume that D2 in the MBH was not induced by hypothyroidism, but rather, it may have been influenced by a unique set of regulatory controls. Support for this hypothesis is given by our previous studies, which showed that only a modest 1.3-fold increase in D2 mRNA can be achieved in the MBH in association with even severe hypothyroidism (4). The tendency for D2 mRNA to be particularly abundant in the palisade zone of the median eminence further suggests that some tanycytes may be particularly susceptible to the effects of LPS. Indeed, at least two distinct subtypes of tanycytes have been identified in the third ventricle based on morphological criteria, including α and β tanycytes (21), although other subtypes are also likely to exist (21, our personal observations).

The recent demonstration of TNF-1 receptor (p55) mRNA in tanycytes in normal rats and its increase by endotoxin administration (7) and the ability of TNF-α to increase endogenous D2 activity in GH3 cells in culture (22) support the concept that LPS or LPS-induced proinflammatory cytokines could directly activate D2 in tanycytes in the MBH. Because NF-κB plays a key role in the signaling of LPS, TNF, and other cytokine receptors (9, 10, 23) and because by computer analysis using the Transcription Element Search Software (TESS; http://www.cbil.upenn.edu/tess; University of Pennsylvania, Philadelphia, PA), the 6.9-kb 5′FR region of h*dio*2 promoter may contain multiple putative NF-κB binding sites, we determined whether the *dio*2 gene can be activated by the NF-κB second messenger system.

Coexpression of the p65 subunit of the activated NF-κB heterodimer together with a 6.5-kb h*dio*2 5′FR CAT construct resulted in an approximately 56-fold increase in the transcriptional activity of h*dio*2 in HEK-293 cells and a remarkable 152-fold increase in HC11 cells. This marked induction of the *dio*2 promoter activity could be decreased by truncation of the promoter to smaller 3′ fragments, both in HEK-293

cells and HC11 cells, and could be completely abolished when p65 was overexpressed together with a 83-bp minimal promoter lacking all putative NF-κB binding sites. The data, therefore, support the concept that NF-κB may be a key mediator of the effects of LPS on the *dio*2 gene in tanycytes, and probably via more than just one NF-κB binding site. This concept would be in keeping with evidence that NF-κB is activated in the median eminence and wall of the third ventricle after LPS administration (24), although the precise cell types have not yet been identified. Additional observations that *dio*2 could not be activated by TNF-α in mesothelioma (MSTO-211H) (25) and osteoblast-like cells (MC3T3-E1) (our personal observations) would indicate that cytokine induction of D2 activity may be cell-type specific, possibly due to the expression of factors in these cells that are necessary to transduce immune responses.

In contrast to the h*dio*2 promoter, coexpression of p65 with a 3.6-kb r*dio*2-Luc construct in HC11 cells resulted in a lesser but still substantial 2.9-fold induction of the promoter. This difference in responsiveness of h*dio*2 and r*dio*2 to p65 could be due to a different number of functional NF-κB binding sites in the FR of these two genes. The hypothesis is supported by a TESS search (combined string and weight matrix search, maximum allowable string mismatch: 15%), which indicates multiple putative NF-κB binding sites in the h*dio*2 but only one in the r*dio*2 FR. The functional importance of these predicted binding sites, however, will require confirmation by *in vitro* assays.

The importance of immune activation of D2 in tanycytes may lie in the potential role of D2 in mediating central hypothyroidism that can occur during infection. In man, this disorder is commonly referred to as the nonthyroidal illness syndrome (26, 27), which is presumably an important homeostatic mechanism that allows for energy conservation during severe illness (26, 27). Contrary to the mechanism of central hypothyroidism associated with fasting (28–31), infection increases the gene expression of proopiomelanocortin in arcuate nucleus neurons (32), perhaps as a necessary response to prevent severe hyperthermia (33), increases cocaine- and amphetamine-regulated transcript (CART) gene

expression (32), does not increase neuropeptide Y (NPY) expression (32), elevates circulating levels of leptin (34), and increases norepinephrine release (35). Collectively, these responses would predict an increase in TRH gene expression in hypophysiotropic neurons rather than a suppression as observed (36, 37). Presumably, therefore, a more potent, overriding inhibitory influence mediated by mechanisms other than those described above for fasting becomes activated during infection, superceding any stimulatory action of leptin, α-MSH, CART, and/or catecholamines on the hypothalamic-pituitary-thyroid axis. This overriding effect does not appear to be due to increased level of glucocorticoids because adrenalectomized animals replaced with corticosterone to simulate normal basal levels still show suppression of TRH and TRH mRNA after LPS (36).

Therefore, we propose that, during infection, LPS or LPS-induced proinflammatory cytokines exert a direct action to stimulate the synthesis of D2 in tanycytes of the MBH. We hypothesize that the ensuing MBH-specific D2-mediated thyrotoxicosis caused by increased T_4 to T_3 conversion in tanycytes may suppress the synthesis of TRH in hypophysiotropic neurons. This may occur by local feedback inhibition through the release of T_3 from tanycyte apical processes into the CSF or uptake from hypophysiotropic TRH axonal processes in the median eminence and retrograde transport to the hypothalamic PVN. T_3 may also be released into the hypophysial portal system from tanycyte endfeet processes for conveyance to the anterior pituitary and exert direct effects on thyrotropes to inhibit the secretion of TSH.

Acknowledgments

References

1. **Bianco AC, Salvatore D, Gereben B, Berry MJ, Larsen PR** 2002 Biochemistry, cellular and molecular biology, and physiological roles of the iodothyronine selenodeiodinases. Endocr Rev 23:38–89
2. **Kakucska I, Rand W, Lechan RM** 1992 Thyrotropin-releasing hormone gene expression in the hypothalamic paraventricular nucleus is dependent upon feedback regulation by both triiodothyronine and thyroxine. Endocrinology 130:2845–2850
3. **Schneider MJ, Fiering SN, Pallud SE, Parlow AF, St. Germain DL, Galton VA** 2001 Targeted disruption of the type 2 selenodeiodinase gene (Dio2) results in a phenotype of pituitary resistance to T4. Mol Endocrinol 15:2137–2148
4. **Tu HM, Kim SW, Salvatore D, Bartha T, Legradi G, Larsen PR, Lechan RM** 1997 Regional distribution of type 2 thyroxine deiodinase messenger ribonucleic acid in rat hypothalamus and pituitary and its regulation by thyroid hormone. Endocrinology 138:3359–3368
5. **Bruni JE** 1974 Scanning and transmission electron microscopy of the ependymal lining of the third ventricle. Can J Neurol Sci 1:59–73
6. **Krisch B, Leonhardt H, Buchheim W** 1978 The functional and structural border between the CSF- and blood-milieu in the circumventricular organs (organum vasculosum laminae terminalis, subfornical organ, area postrema) of the rat. Cell Tissue Res 195:485–497
7. **Nadeau S, Rivest S** 1999 Effects of circulating tumor necrosis factor on the neuronal activity and expression of the genes encoding the tumor necrosis factor receptors (p55 and p75) in the rat brain: a view from the blood-brain barrier. Neuroscience 93:1449–1464
8. **Nishibori M, Nakaya N, Mori S, Saeki K** 1997 Immunohistochemical localization of macrophage migration inhibitory factor (MIF) in tanycytes, subcommissural organ and choroid plexus in the rat brain. Brain Res 758:259–262
9. **Hanada T, Yoshimura A** 2002 Regulation of cytokine signaling and inflammation. Cytokine Growth Factor Rev 13:413–421
10. **Li Q, Verma IM** 2002 NF-κB regulation in the immune system. Nat Rev Immunol 2:725–734
11. **Fekete C, Kelly J, Mihály E, Sarkar S, Rand WM, Légrádi G, Emerson CH, Lechan RM** 2001 Neuropeptide Y has a central inhibitory action on the hypothalamic-pituitary-thyroid axis. Endocrinology 142:2606–2613
12. **Curcio C, Baqui MM, Salvatore D, Rihn BH, Mohr S, Harney JW, Larsen PR, Bianco AC** 2001 The human type 2 iodothyronine deiodinase is a selenoprotein highly expressed in a mesothelioma cell line. J Biol Chem 276:30183–30187
13. **Bartha T, Kim SW, Salvatore D, Gereben B, Tu HM, Harney JW, Rudas P, Larsen PR** 2000 Characterization of the 5'-flanking and 5'-untranslated regions of the cyclic adenosine 3', 5'-monophosphate-responsive human type 2 iodothyronine deiodinase gene. Endocrinology 141:229–237
14. **Gereben B, Salvatore D, Harney JW, Tu HM, Larsen PR** 2001 The human, but not rat, dio2 gene is stimulated by thyroid transcription factor-1 (TTF-1). Mol Endocrinol 15:112–124
15. **Geymayer S, Doppler W** 2000 Activation of NF-κB p50/p65 is regulated in the developing mammary gland and inhibits STAT5-mediated β-casein gene expression. FASEB J 14:1159–1170
16. **Boussif O, Lezoualc'h F, Zanta MA, Mergny MD, Scherman D, Demeneix B, Behr JP** 1995 A versatile vector for gene and oligonucleotide transfer into cells in culture and in vivo: polyethylenimine. Proc Natl Acad Sci USA 92:7297–7301
17. **Wolff B, Naumann M** 1999 INK4 cell cycle inhibitors direct transcriptional inactivation of NF-κB. Oncogene 18:2663–2666
18. **Brent GA, Larsen PR, Harney JW, Koenig RJ, Moore DD** 1989 Functional characterization of the rat growth hormone promoter elements required for induction by thyroid hormone with and without a co-transfected β type thyroid hormone receptor. J Biol Chem 264:178–182
19. **Seed B, Sheen JY** 1988 A simple phase-extraction assay for chloramphenicol acyltransferase activity. Gene 67:271–277
20. **Toyoda N, Harney JW, Berry MJ, Larsen PR** 1994 Identification of critical amino acids for 3, 5, 3'-triiodothyronine deiodination by human type 1 deiodinase based on comparative functional-structural analyses of the human, dog, and rat enzymes. J Biol Chem 269:20329–20334
21. **Akmayev IG, Fidelina OV, Kabolova ZA, Popov AP, Schitkova TA** 1973 Morphological aspects of the hypothalamic-hypophyseal system. IV. Medial basal hypothalamus. An experimental morphological study. Z Zellforsch Mikrosk Anat 137:493–512
22. **Baur A, Bauer K, Jarry H, Kohrle J** 2000 Effects of proinflammatory cytokines on anterior pituitary 5'-deiodinase type I and type II. J Endocrinol 167:505–515
23. **Laflamme N, Rivest S** 2001 Toll-like receptor 4: the missing link of the cerebral innate immune response triggered by circulating gram-negative bacterial cell wall components. FASEB J 15:155–163
24. **Nadeau S, Rivest S** 2000 Role of microglial-derived tumor necrosis factor in mediating CD14 transcription and nuclear factor κB activity in the brain during endotoxemia. J Neurosci 20:3456–3468
25. **Curcio C, Baqui MMA, Salvatore D, Rihn BH, Mohr S, Harney JW, Larsen PR, Bianco AC** 2001 The human type 2 iodothyronine deiodinase is a selenoprotein highly expressed in a mesothelioma cell line. J Biol Chem 276: 30183–30187
26. **De Groot LJ** 1999 Dangerous dogmas in medicine: the nonthyroidal illness syndrome. J Clin Endocrinol Metab 84:151–164
27. **Larsen PR, Davies TF, Schlumberger MJ, Hay ID** 2002 Thyroid physiology and diagnostic evaluation of patients with thyroid disorders. In: Polonsky KS, ed. Williams textbook of endocrinology. 10th ed. Philadelphia: Saunders; 350–352
28. **Légrádi G, Emerson CH, Ahima RS, Flier JS, Lechan RM** 1997 Leptin prevents fasting-induced suppression of prothyrotropin-releasing hormone messenger ribonucleic acid in neurons of the hypothalamic paraventricular nucleus. Endocrinology 138:2569–2576
29. **van Haasteren GAC, Linkels E, Klootwijk W, van Toor H, Rondeel JMM, Themmen APN, de Jong FH, Valentijn K, Vaudry H, Bauer K, Visser TJ, de Greef WJ** 1995 Starvation-induced changes in the hypothalamic content of prothyrotrophin-releasing hormone (proTRH) mRNA and the hypothalamic release of proTRH-derived peptides: role of the adrenal gland. J Endocrinol 145:143–153
30. **Rondeel JM, Heide R, de Greef WJ, van Toor H, van Haasteren GA, Klootwijk W, Visser TJ** 1992 Effect of starvation and subsequent refeeding on thyroid function and release of hypothalamic thyrotropin-releasing hormone. Neuroendocrinology 56:348–353
31. **Fekete C, Légrádi G, Mihály E, Huang QH, Tatro JB, Rand WM, Emerson CH, Lechan RM** 2000 α-Melanocyte-stimulating hormone is contained in nerve terminals innervating thyrotropin-releasing hormone-synthesizing neurons in the hypothalamic paraventricular nucleus and prevents fasting-induced suppression of prothyrotropin-releasing hormone gene expression. J Neurosci 20:1550–1558

32. **Sergeyev V, Broberger C, Hokfelt T** 2001 Effect of LPS administration on the expression of POMC, NPY, galanin, CART and MCH mRNAs in the rat hypothalamus. Brain Res Mol Brain Res 90:93–100

33. **Huang QH, Entwistle ML, Alvaro JD, Duman RS, Hruby VJ, Tatro JB** 1997 Antipyretic role of endogenous melanocortins mediated by central melanocortin receptors during endotoxin-induced fever. J Neurosci 17:3343–3351

34. **Grunfeld C, Zhao C, Fuller J, Pollack A, Moser A, Friedman J, Feingold KR** 1996 Endotoxin and cytokines induce expression of leptin, the ob gene product, in hamsters. J Clin Invest 97:2152–2157

35. **Francis J, MohanKumar SM, MohanKumar PS** 2000 Correlations of norepinephrine release in the paraventricular nucleus with plasma corticosterone and leptin after systemic lipopolysaccharide: blockade by soluble IL-1 receptor. Brain Res 867:180–187

36. **Kondo K, Harbuz MS, Levy A, Lightman SL** 1997 Inhibition of the hypothalamic-pituitary-thyroid axis in response to lipopolysaccharide is independent of changes in circulating corticosteroids. Neuroimmunomodulation 4:188–194

37. **Kakucska I, Romero LI, Clark BD, Rondeel JM, Qi Y, Alex S, Emerson CH, Lechan RM** 1994 Suppression of thyrotropin-releasing hormone gene expression by interleukin-1-β in the rat: implications for nonthyroidal illness. Neuroendocrinology 59:129–137